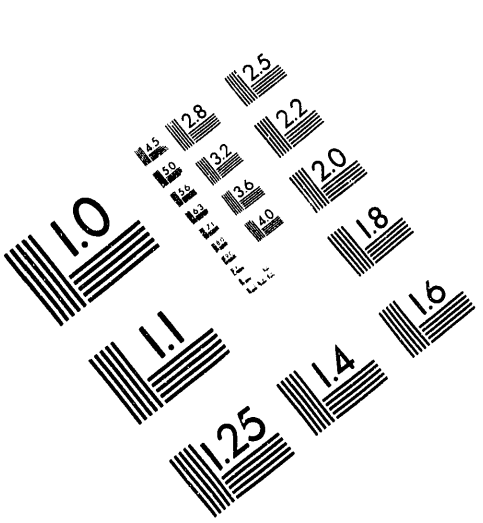

Association for Information and Image Management
1100 Wayne Avenue, Suite 1100
Silver Spring, Maryland 20910
301/587-8202

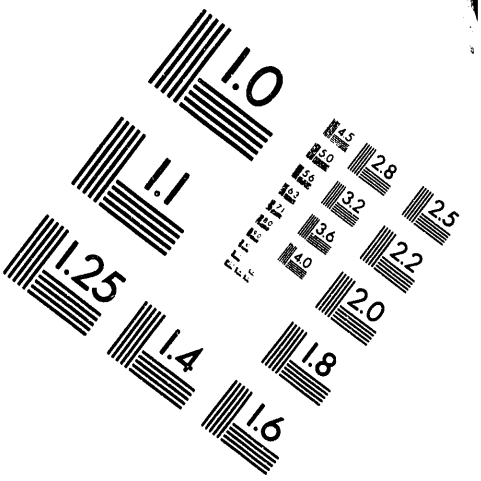

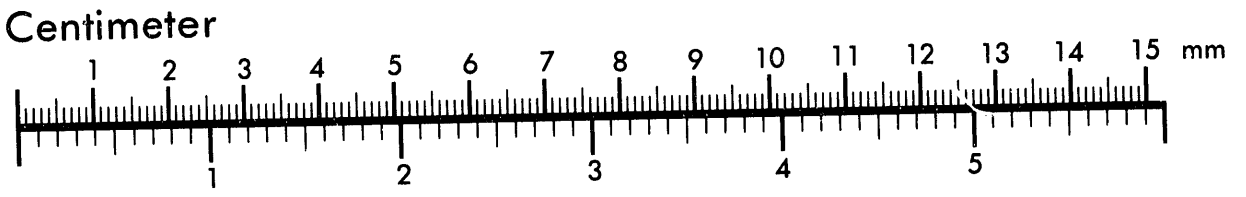

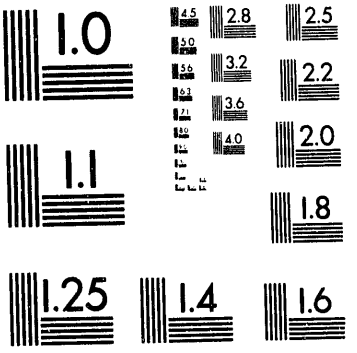

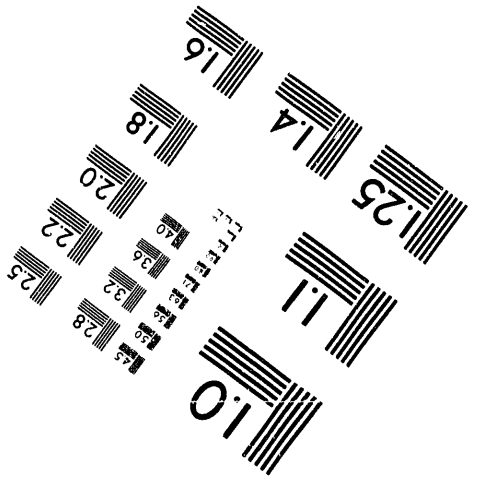

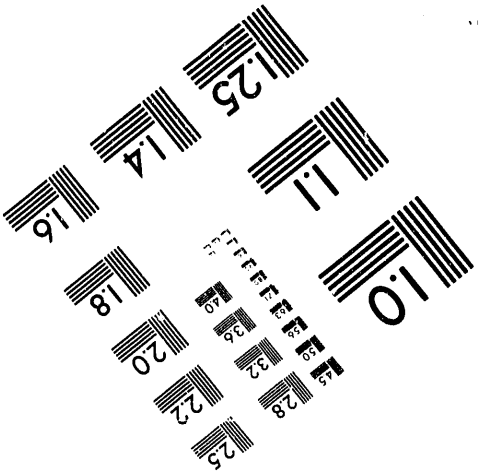

MANUFACTURED TO AIIM STANDARDS
BY APPLIED IMAGE, INC.

1 of 1

Submitted to ICAS Conference Malente/Hamburg Germany
August 17-21, 1992

Suppression of Charge Scattering in Mössbauer Experiments using Synchrotron Radiation

U. Bergmann[a] , D. P. Siddons and J. B. Hastings

NSLS, Brookhaven National Laboratory, Upton, New York 11973

1. INTRODUCTION

The extremely small ratio of linewidth to energy ($\Gamma/E \simeq 10^{-10} - 10^{-17}$) combined with the character of recoil free absorption and reemission (Mössbauer effect) makes the low lying nuclear resonances a unique spectroscopic tool. Further, considering the simplicity of performing Mössbauer experiments, they have become very useful in a wide range of disciplines. ^{57}Fe has remained the most widely used isotope despite its low natural abundance (2%) because iron is ubiquitous in nature and shows a strong effect. The energy width of this resonance corresponds to a lifetime of 140 *nsec* of the excited state. Therefore in principle time differential spectroscopy is possible. Already in 1960, shortly after the discovery of ^{57}Fe as a Mössbauer isotope, a time dependent measurement was performed [1]. Using the time differential measurement one is no longer restricted to a nuclear source (narrow in energy), in fact a short pulse (and therefore broad energy band) excitation is favored in such experiments. The concept of using a pulsed source and time gating to isolate the resonant scattering was already suggested in 1962 [2]. In 1974 it was noted that synchrotron radiation (SR) was ideally suited to this task [3]. Although the time gating technique is conceptually simple the bandwidth of SR ($\Delta E/E \simeq 1$) poses significant technical difficulties.

In this paper we will discuss the extraction of the nuclear signal from the overwhelming background, which is the central problem in SR-based Mössbauer experiments. We will only consider the ^{57}Fe-isotope, although other isotopes might be of interest in a SR-based experiment (see for example [4]). Although SR sources have the disadvantages of creating this high background and being limited in beam-time and location, new and unique opportunities make them very attractive even with these difficulties. For this reason research and development groups at every major SR facility worldwide are increasingly working on Mössbauer experiments, stimulated by the first successful observation of nuclear Bragg scattering (NBS) using SR in 1984 [5].

In addition to the obvious advantage of increased brightness provided by a SR-source qualitatively new experiments become possible. The reason for this is the form of the SR-excitation. The short, broad band SR pulse intrinsically provides a coherent excitation

*Work performed under the auspices of the U.S. Department of Energy, under contract DE-AC02-76CH00016.

which is distributed over the whole ensemble of nuclei (exciton). The deexcitation is also coherent in both nuclear forward scattering (NFS) and NBS. This form of excitation favors a time measurement of the decaying state, which is connected to an absorption measurement by Fourier transformation and Kramers Kronig relation. The decay time of the ensemble depends on the number of nuclear scatterers per unit area, with its upper limit given by the natural lifetime for a single nucleus. The decay also depends in detail on the Lamb-Mössbauer factor and abundance as well as the nuclear parameters such as conversion coefficient, magnetic and quadrupole splittings and, in special arrangements, isomeric shifts. It is important to note, that the state prepared with SR is different from the one using the ^{57}Co source. The short SR pulse has a transit time through the sample much smaller than the lifetime which allows the system to decay freely. This effect, which is interesting in its own right greatly facilitates the analysis since no source effects have to be considered. Choosing a long time between excitation pulses (this depends on the geometry of the SR facility but is in general possible) can in principle allow a more precise determination of the hyperfine parameters. Important in this context is the phenomenon of quantum-beats, predicted in 1977 [6] and first observed in 1986 [7]. Quantum beats are the time analog to energy splittings. In a long time window one can consider many beats in the fitting procedure and therefore determine the beat frequency and shape more precisely than the lineshape and splitting in an absorption measurement.

Even with all the advantages of SR compared to a conventional source there is no guarantee that SR-based Mössbauer experiments will become routine and a useful tool for many researchers. This will depend on how conveniently the experiment and analysis can be performed. So far only one user application has been reported [8]. The main reasons for this are the large background and the lack of availability of intense (insertion device) SR sources. Since the intensity problem is about to be solved by the third generation SR sources, the reduction of the background remains the crucial problem to be addressed. The difficulty can be easily understood by the following estimate. The best possible monochromatization using a Si monochromator leads to an energy width of some meV, which is 10^6 times broader than the natural linewidth of ^{57}Fe. For observing delayed resonant intensities with total incident fluxes above 10^6 Hz existing detectors are not well behaved. Therefore background supression is required.

2. SUPPRESSION BY RESONANT FILTERING

2.1. Pure nuclear Bragg scattering

All of the first SR-based Mössbauer experiments used NBS from crystals enriched with ^{57}Fe [5], [10], [9]. The geometry was chosen to use a charge forbidden pure nuclear Bragg reflection. The suppression depends on the crystal perfection and the bandwidth of the incoming SR-pulse. The best published ratio of signal to noise (100 to 1) was achieved by the combination of a Fe_2O_3 crystal combined with a high resolution Si-monochromator using four consecutive (10 6 4) reflections [11]. NBS has been used very successfully. For example the first observation of the the quantum beats [7], the speedup of the coherent

nuclear decay [9] and the first direct observation of polarization mixing [12] were all demonstrated with pure NBS. Several other experiments have been and are currently being performed.

However this technique has some disadvantages. First, the production of these crystals is often expensive and difficult. Only a few such crystals exist worldwide. Furthermore the ill-defined crystal perfection complicates the analysis. Using such a crystal as a resonant filter in front of a nuclear scatterer, for example NFS of an ^{57}Fe-containing sample makes the analysis problem even more severe. The measured time evolution depends now on both the sample and the enriched crystal filter and has consequently to be deconvolved. The energy band provided by such a crystal has a significant structure and its width is comparable to that of a typical sample. As a consequence the excitation is no longer broadband and one of the main advantages of SR, the decoupling of the source and sample, is removed. Nevertheless charge forbidden NBS as a suppression possibility is a very powerful technique, especially if the application uses the crystal itself as the sample.

2.2. Reflection from GIAR-films

Another resonant filter device which can be used to suppress the nonresonant background is a GIAR-film (GIAR = grazing incidence anti reflection). GIAR-films, which use destructive interference of reflected x-rays to achieve the charge suppression, are nuclear filters which can provide an energy band up to several hundred times the natural linewidth Γ. However the suppression of the nonresonant radiation is limited by surface and interface roughness of the mirror system and by beam divergence. Broad filters (ΔE greater than 160 Γ) are desirable since they cover the energy range of hyperfine splittings in ^{57}Fe containing samples. To achieve these bandwidths very small reflecting angles are needed which magnify the sensitivity to surface and interface roughness and beam divergence. The best suppression of electronic reflectivity reported to date is a factor of 25 for a GIAR-film reflecting a 100 Γ bandwidth [13]. In this experiment the relative suppression (charge to nuclear), was a factor 10. Technical improvements in the production of GIAR-films are possible which may lead to a relative suppression of the order of hundred. Even this suppression is not enough to fully utilize the third generation sources, although the use of several consecutive films could possibly improve the suppression. However, a GIAR-film introduces significant spectral variations within its bandpass. Most notable is the strong reflectivity minimum directly below the resonance energy. For some samples the influence of these features can be avoided. In this case the GIAR-film can provide a fairly uniform excitation of all hyperfine split levels in the sample. For many samples of interest this is not the case and in general one looses information. For example, if the sample has no resolved splittings but only a broadening this problem can become severe since the level partly coincides with the stong minimum of the reflected band. Using a GIAR-film to suppress charge scattering therefore complicates the experiment and/or the analysis.

In conclusion, charge suppression provided by resonant filters, inevitably introduces complications in the perfomance of SR-based Mössbauer experiments. However it is useful in certain cases, especially where it is the only suppression possibility so far.

3. SUPRESSION USING CROSSED POLARIZERS

3.1. Supression principle

A different approach to achieve charge suppression without a resonant filter is based on polarization phenomena related to the nuclear transitions of ^{57}Fe [14]. The idea is to place the resonant sample between two crossed polarizers. Then, only a polarization mixing in the scattering process leading to a componenent which is 90° rotated, will result in a signal. This technique utilizes the intrinsically high degree of polarization and the brightness of SR to its fullest.

Figure (1) shows the schematic geometry of such an experiment. The equation in the figure is based on a formalism in which the sample is described by a frequency dependent transmission matrix $\tilde{T}(\omega)$ to be discussed in detail in section 3.2. The polarizers are described by Jones-matrices (see for example [15]). Incoming and outgoing amplitudes are represented by Jones-vectors, where the two components represent different polarization states. In this convention σ-polarization is given by the basis vector (1,0) and π-polarization by the basis vector (0,1).

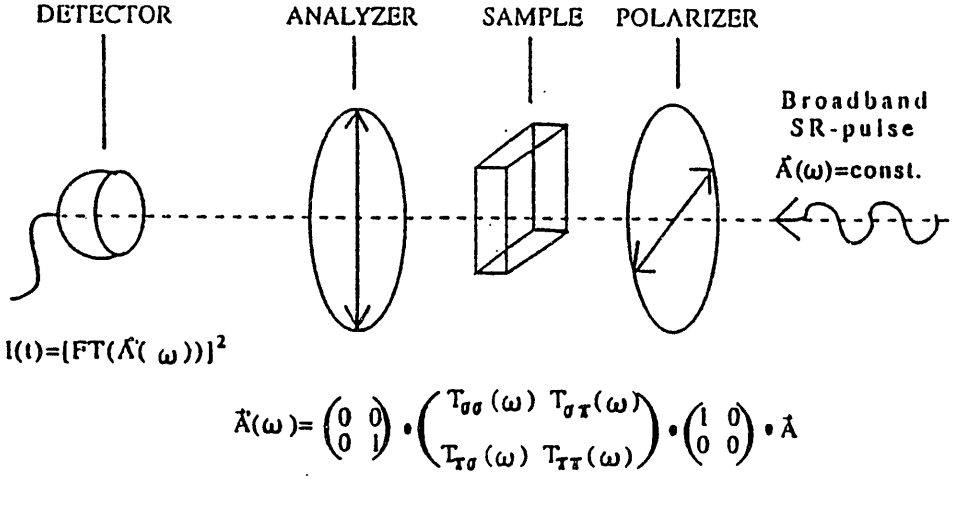

FIGURE 1. The two crossed polarizers lead to a suppression if the sample shows no polarization mixing. The sample is characterized by the transmission matrix $\tilde{T}(\omega)$. Only the matrix element $T_{\pi\sigma}(\omega)$ is probed in the given geometry.

From the equation in Figure (1) it can immediately be seen that, ideally, only an off diagonal element in the transmission matrix (which corresponds to polarization mixing) can contribute to the signal in the detector. The prompt background radiation however does not show any rotation and hence is suppressed by the crossed polarizers. Previous work [16] has demonstrated that a pefect-crystal polarimeter in the crossed setting is capable of suppressions of the order of 10^6. Such perfect crystal polarimeters are well matched to undulator sources on third generation facilities because of the significant collimation requirements in both vertical and horizontal planes. In contrast, current bending magnet sources are optically highly anisotropic and hence the use of such a polarimeter results in substantial intensity loss. The demonstration experiment which we describe here was performed on a dipole source at NSLS and therefore involves some compromise in the polarization analyzer (crossed polarizer) adopted.

3.2. Evaluation of the Transmission Matrix $\tilde{T}(\omega)$

The theoretical treatment of the transmission of radiation through a Mössbauer absorber has been previously discussed by several authors [17, 18, 19, 20]. The unpublished work [20] gives perhaps the best connection between theory and our experiment and forms the basis for the analysis presented below. For clarity we consider the case of a single ^{57}Fe site including all hyperfine splittings. This formalism can easily be extended to multiple sites and other isotopes. Consistent with the formalism generally used in optics, NFS can be described by characterizing the resonant medium with a complex index of refraction expressed as a frequency dependent 2x2 matrix $\tilde{n}(\omega)$. However, there is no direct way to measure $\tilde{n}(\omega)$. In our experiment we measure the transmitted intensity as a function of time $I(t)$. The connection between $I(t)$ and $\tilde{n}(\omega)$ is easily seen through the calculation of a transmission matrix $\tilde{T}(\omega)$ (see Fig. (1)), which gives the response of the sample as a function of frequency. We show how $\tilde{T}(\omega)$ is related to $I(t)$ and further how $\tilde{T}(\omega)$ depends on the nuclear transition amplitudes $F_i(\omega)$, which contain all the parameters of interest. In this derivation a linear polarization basis which is appropriate for SR is used.

Consider the solution of the wave equation in a dispersive medium. The transmitted electromagnetic field can be written as

$$\vec{A}'(\omega) = e^{(i\cdot\tilde{n}(\omega)\cdot k_0\cdot d)} \cdot \vec{A}(\omega). \tag{1}$$

In this expression d represents the sample thickness, k_0 the wave vector in vacuum and $\tilde{n}(\omega)$ is given by

$$\tilde{n}(\omega) = 1 + \lambda\!\!\!^{-} \cdot \tilde{f}(\omega), \tag{2}$$

with $\lambda\!\!\!^{-}$ the wavelength over 2π in vacuum and

$$\tilde{f}(\omega) = \begin{pmatrix} f_{\sigma\sigma}(\omega) & f_{\sigma\pi}(\omega) \\ f_{\pi\sigma}(\omega) & f_{\pi\pi}(\omega) \end{pmatrix}, \tag{3}$$

where the matrix elements represent the coherent nuclear forward scattering amplitudes for a single atom. The subscripts ij of the forward scattering amplitudes refer to the polarizations of emitted and absorbed photon respectively. To evaluate the exponential in equation (1), we express $\tilde{f}(\omega)$ in terms of Pauli matrices defined as

$$\vec{\sigma} = (\sigma_x, \sigma_y, \sigma_z) = \left(\begin{pmatrix} 0 & 1 \\ 1 & 0 \end{pmatrix}, \begin{pmatrix} 0 & -i \\ i & 0 \end{pmatrix}, \begin{pmatrix} 1 & 0 \\ 0 & -1 \end{pmatrix} \right), \tag{4}$$

and write

$$\tilde{f}(\omega) = a + \vec{b} \cdot \vec{\sigma}. \tag{5}$$

From equation (5) it follows directly that

$$\begin{aligned} a &= \frac{1}{2} \cdot (f_{\sigma\sigma}(\omega) + f_{\pi\pi}(\omega)) \\ b_x &= \frac{1}{2} \cdot (f_{\sigma\pi}(\omega) + f_{\pi\sigma}(\omega)) \\ b_y &= \frac{i}{2} \cdot (f_{\sigma\pi}(\omega) - f_{\pi\sigma}(\omega)) \\ b_z &= \frac{1}{2} \cdot (f_{\sigma\sigma}(\omega) - f_{\pi\pi}(\omega)). \end{aligned} \tag{6}$$

By writing $\vec{b} = b \cdot \hat{b}$ with

$$b = \sqrt{b_x^2 + b_y^2 + b_z^2} = \sqrt{\frac{1}{4} \cdot (f_{\sigma\sigma}(\omega) - f_{\pi\pi}(\omega))^2 + f_{\pi\sigma}(\omega) \cdot f_{\sigma\pi}(\omega)}. \tag{7}$$

and using the identity $(\hat{b} \cdot \vec{\sigma})^2 = 1$ (the unit matrix) one can expand $e^{(i \cdot b \cdot \hat{b} \cdot \vec{\sigma} \cdot z)}$ in a Taylor series and rearrange the even and odd powers to get

$$e^{(i \cdot b \cdot \hat{b} \cdot \vec{\sigma} \cdot z)} = cos(b \cdot z) + i(\hat{b} \cdot \vec{\sigma}) \cdot sin(b \cdot z). \tag{8}$$

Putting this result into equation (1) with the use of equations (2),(3) and (5) yields

$$\vec{A}'(\omega) = e^{(i(k_0+a) \cdot d)} \cdot \begin{pmatrix} cos(b \cdot d) + \frac{i}{b} b_z sin(b \cdot d) & \frac{i}{b}(b_x - i \cdot b_y) sin(b \cdot d) \\ \frac{i}{b}(b_x + i \cdot b_y) sin(b \cdot d) & cos(b \cdot d) - \frac{i}{b} b_z sin(b \cdot d) \end{pmatrix} \cdot \vec{A}(\omega). \tag{9}$$

This can be rewritten in the form

$$\begin{pmatrix} A'_\sigma(\omega) \\ A'_\pi(\omega) \end{pmatrix} = e^{(i \cdot k_0 \cdot d)} \cdot \begin{pmatrix} T_{\sigma\sigma}(\omega) & T_{\sigma\pi}(\omega) \\ T_{\pi\sigma}(\omega) & T_{\pi\pi}(\omega) \end{pmatrix} \cdot \begin{pmatrix} A_\sigma(\omega) \\ A_\pi(\omega) \end{pmatrix}. \tag{10}$$

The matrix elements $T_{ij}(\omega)$ are given from those in equation (9) multiplied by $e^{(i\cdot a\cdot d)}$ and the vectors are expressed in our chosen linear basis. The factor $e^{(i\cdot k_0\cdot d)}$ only contributes a phase shift since k_0 is real. It is not measurable in our setup and can hence be neglected. In particular eq. (10) is very convenient since the operator $e^{(i\cdot\hat{n}(\omega)\cdot k_0\cdot d)}$ from eq. (1) is expressed as a matrix. The elements $T_{ij}(\omega)$ of this matrix depend explicitly on the matrix elements $f_{ij}(\omega)$ through eqs. (6), (7) and (9).

In the calculation of these matrix elements, $f_{ij}(\omega)$, we use the dot products of unit vectors representing different directions in the system. $\hat{\pi}$ and $\hat{\sigma}$ give the polarization directions of the photons, $\hat{B}$ is the direction of the internal magnetic field (sample quantization axis) and $\hat{k}_0$ is the direction of the incident wave vector. These products can easily be expressed in terms of the polar angle θ and the azimuthal angle ϕ, where θ is the angle between $\hat{k}_0$ and $\hat{B}$, and ϕ is the angle between the projection of $\hat{B}$ in the plane perpendicular to $\hat{k}_0$ and $\hat{\sigma}$. The matrix elements f_{ij} can then be written in the following form,

$$f_{\sigma\sigma}(\omega) = \tfrac{3\pi}{2}\rho\lambda\!\!\!^{-2}[F_1(\omega) + F_{-1}(\omega) + (\hat{\pi}\cdot\hat{B})^2(2F_0(\omega) - F_1(\omega) - F_{-1}(\omega))]$$

$$f_{\sigma\pi}(\omega) = \tfrac{3\pi}{2}\rho\lambda\!\!\!^{-2}[-i(\hat{k}_0\cdot\hat{B})(F_1(\omega) - F_{-1}(\omega)) - (\hat{\sigma}\cdot\hat{B})(\hat{\pi}\cdot\hat{B})(2F_0(\omega) - F_1(\omega) - F_{-1}(\omega))]$$

$$f_{\pi\sigma}(\omega) = \tfrac{3\pi}{2}\rho\lambda\!\!\!^{-2}[i(\hat{k}_0\cdot\hat{B})(F_1(\omega) - F_{-1}(\omega)) - (\hat{\sigma}\cdot\hat{B})(\hat{\pi}\cdot\hat{B})(2F_0(\omega) - F_1(\omega) - F_{-1}(\omega))]$$

$$f_{\pi\pi}(\omega) = \frac{3\pi}{2}\rho\lambda\!\!\!^{-2}[(F_1(\omega) + F_{-1}(\omega)) + (\hat{\sigma}\cdot\hat{B})^2(2F_0(\omega) - F_1(\omega) - F_{-1}(\omega))]. \qquad (11)$$

In this equation ρ is the density of nuclei and $F_0(\omega)$, $F_1(\omega)$, $F_{-1}(\omega)$ are the nuclear transition amplitudes for photon processes with $\Delta m = 0, \pm 1$. For the six possible transitions of the ^{57}Fe nucleus they are

$$\begin{aligned}
F_0 &= f\cdot p\cdot\frac{1}{2j_0+1}\cdot\frac{1}{1+\alpha}\cdot\left(\frac{2/3}{\Delta\omega_2-\omega-i}+\frac{2/3}{\Delta\omega_5-\omega-i}\right)\\
F_1 &= f\cdot p\cdot\frac{1}{2j_0+1}\cdot\frac{1}{1+\alpha}\cdot\left(\frac{1}{\Delta\omega_1-\omega-i}+\frac{1/3}{\Delta\omega_4-\omega-i}\right)\\
F_{-1} &= f\cdot p\cdot\frac{1}{2j_0+1}\cdot\frac{1}{1+\alpha}\cdot\left(\frac{1}{\Delta\omega_6-\omega-i}+\frac{1/3}{\Delta\omega_3-\omega-i}\right)
\end{aligned} \qquad (12)$$

with the Lamb-Mössbauer factor f, the ^{57}Fe abundance p, the groundstate spin $j_0 = 1/2$ and the conversion coefficient α. The terms inside the brackets contain the transition strengths (Clebsch-Gordon coefficients) in the numerator and the hyperfine splittings $\Delta\omega_i$ numbered in the usual convention in the denominator. All frequencies in the denominator are dimensionless and have to be considered in units of $\Gamma/2$.

To include the charge part in the forward scattering amplitudes one has to add $f_e = f_0 + i\cdot f'$ to the diagonal elements $f_{\sigma\sigma}(\omega)$ and $f_{\pi\pi}(\omega)$. The real part, f_0, only contributes a phase shift and can be neglected. The imaginary part, f', leads to a decrease of the transmitted amplitude by a factor $e^{(-f'\cdot d)}$. Although $i\cdot f'$ only contributes to the diagonal elements of $\bar{f}(\omega)$, it is present in all matrix elements $T_{ij}(\omega)$ through the factor

$e^{(i \cdot a \cdot d)}$. This is consistent with the fact that electronic absorption has to reduce the intensity in both the unrotated scattering given by $T_{\sigma\sigma}(\omega)$ and $T_{\pi\pi}(\omega)$ as well as 90° rotated scattering given by $T_{\sigma\pi}(\omega)$ and $T_{\pi\sigma}(\omega)$. Each matrix element $T_{ij}(\omega)$ represents the polarization dependent response of the whole system of scatterers, whereas each $f_{ij}(\omega)$ considers only a single atom. In the case, where each atom scatters without change of polarization, i.e. $\tilde{f}(\omega)$ is diagonal, the response $\tilde{T}(\omega)$ of the whole system also doesn't change the polarization. $T_{\sigma\pi}(\omega)$ and $T_{\pi\sigma}(\omega)$ are zero as can be seen immediately from eq. (9) and (6), since both, b_x and b_y are zero. In this case our suppression method would not be applicable.

Fom eq. (11) it can be seen under which conditions $\tilde{f}(\omega)$ is diagonal. There are basically three such cases. First, the situation where the quantization axis is parallel to the $\vec{B}$-field of the incoming wave. This corresponds to $\hat{\pi} \cdot \hat{B} = 1$, $\hat{\sigma} \cdot \hat{B} = 0$ and $\hat{k_0} \cdot \hat{B} = 0$. As can be seen in eq. (11), in this case only the $\Delta m = 0$ transitions are excited. Measurements and the corresponding calculation of this special case are given in [21] and in more detail in [22]. Second, the quantization axis is parallel to the $\vec{E}$-field of the incoming wave ($\hat{\sigma} \cdot \hat{B} = 1$, $\hat{\pi} \cdot \hat{B} = 0$ and $\hat{k_0} \cdot \hat{B} = 0$). In this case only the $\Delta m = \pm 1$ transitions are excited. The third case corresponds to the situation where there are no splittings and hence $F_0(\omega) = F_1(\omega) = F_{-1}(\omega)$ which also leads to $f_{\pi\sigma(\omega)} = f_{\sigma\pi(\omega)} = 0$. Any other situation however leads to contributions in the off diagonal elements of $\tilde{T}(\omega)$ and the suppression methods of crossed polarizers can be applied.

In conclusion, the explicit form of the nuclear transition amplitudes given in equation (12) including electronic absorption fully determines $\tilde{T}(\omega)$. It is in general a complex quantity giving the coherent response of a sample of thickness d containing ^{57}Fe nuclei with abundance p to an incoming wave at frequency ω. If the incoming wave has a well defined polarization and its intensity is constant over an energy range large compared to the splittings $\Delta\omega_i$ ($\vec{A}(\omega) = const.$) the time dependent intensity measured is proportional to the modulus squared of the Fourier transformation of the $T_{ij}(\omega)$'s. In a forward scattering Mössbauer experiment using SR both conditions can be fullfilled by using the appropriate monochromator. This allows a straightforward analysis of the sample parameters.

3.3. Experimental setup

The experimental setup is shown in Fig. (2). Ideally, the monochromator should accept the full vertical opening of the SR and provide the best possible energy resolution. At the same time it has to polarize the incident beam. For ^{57}Fe the Si (840) reflection is the best choice for polarization since its Bragg angle is 45.1°. The angular acceptance for symmetric reflection is 0.4 *arcsec* and provides 26 *meV* energy resolution. Neither of these are optimal. However by judicious use of asymmetric cuts and arranging these crystals in the dispersive setting one can get significant improvements in both angular acceptance and energy resolution. For convenience one can utilize two additional symmetric reflections (see Fig. 2) which preserve the gains from the asymmetry and make the geometry much simpler. We chose an asymmetry angle of $-39°$ leading to a three fold increase in acceptance (1.2 *arcsec*) and the same reduction in energy width (8.6 *meV*). It should be noted that the two diffracting surfaces in the asymmetric-symmetric pairs have slightly different Bragg-angles due to refraction. This shift of 0.5 *arcsec* was compensated by bending each

monolith with a spring loaded actuator (see Fig. (2)). Using the nuclear resonance we measured an energy width of 12 meV (compared to the theoretical value of 8.6 meV) for the monochromator. This difference is probably due to a slight misalignment. According to the dynamical diffraction theory the degree of σ-polarization achieved with this crystal system differs from one by a part in 10^{12} . However, this value almost certainly can not be achieved experimentally because of, for example, crystal imperfections and diffuse and multiple scattering.

Ideally, the analyzer would be identical to the polarizer, but the mentioned optical anisotropy of the SR bending magnet source forces a compromise for the analyzer. Therefore we chose the Be (00.6) reflection, which has a Bragg angle of 46.01° and thus poorer polarization properties than the Si (840) reflection. However the slight mosaic spread (20 $arcsec$) provides a significantly larger horizontal acceptance. The crystal used with this small mosaic spread still has good reflectivity.

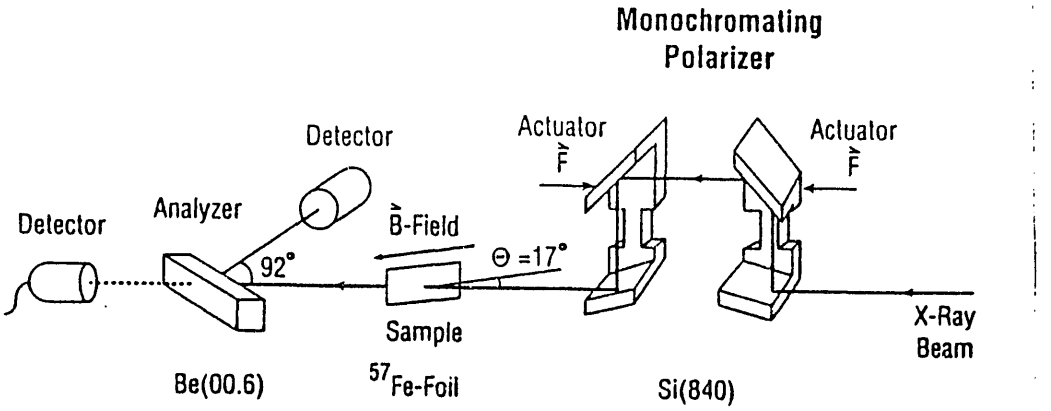

FIGURE 2. The monochromating polarizer improves the σ-polarization of the incident beam. A highly enriched ^{57}Fe sample serves as transmitter, its magnetic field is aligned along the foil which is inclined 17° to the beam to produce a large parallel component. The beryllium crystal serves as a crossed polarizer to suppress unrotated scattering. If the beryllium crystal is taken out of the beam, the detector measures the total intensity in the forward direction.

3.4. Experimental results

To demonstrate the polarization mixing, measurements were made of the time dependent intensity forward scattered from a highly (95%) enriched ^{57}Fe foil. The chosen geometry, where the quantization axis $\hat{B}$ has a large component parallel to $\hat{k}_0$ is known as the Faraday geometry. This corresponds to a small angle θ. For practical reasons we chose $\theta = 17°$ and $\phi = 0$ ($\hat{k}_0 \cdot \hat{B} = 0.956$, $\hat{\sigma} \cdot \hat{B} = 0.292$ and $\hat{\pi} \cdot \hat{B} = 0$). It is clear from equations (11) that the main contribution arises from the $\Delta m = \pm 1$ transitions given by F_1 and F_{-1}. In fact, the amplitude $F_0(\omega)$ only appears in equation (11) because θ (and therefore $\hat{\sigma} \cdot \hat{B}$) is nonzero.

Nuclear Faraday rotation was first observed in 1963 by P. Imbert [23]. Later U. Gonser and R. M. Housley [24] applied it to determine the sign of the internal magnetic field. In Imbert's experiment the polarized incident beam was produced by selective absorption of one polarization of the γ-ray beam from a ^{57}Co source, Doppler shifted to the appropriate line. After transmission through the ^{57}Fe sample, the new polarization was found by rotating the external magnetic field of another absorber (the analyzer) and applying Malus' law. Since the Mössbauer resonance is very narrow, the rotation angle depends on both the sample thickness and frequency of the incoming γ-rays.

Using SR there is an important qualitative difference. Polarization and intensity of the incoming SR pulse are frequency independent and all oscillators are excited coherently. The rotation of the polarization is now independent of thickness. The rotation becomes time dependent with a precession period depending only on the frequency differences $\Delta\omega_4 - \Delta\omega_1$ ($\Delta m = 1$) and $\Delta\omega_6 - \Delta\omega_3$ ($\Delta m = -1$). To illustrate this phenomenon we calculate $\vec{A}'(t)$, which is the Fourier transform of the transmitted amplitude $\vec{A}'(\omega)$ given by

$$\vec{A}'(\omega) = \begin{pmatrix} T_{\sigma\sigma}(\omega) \\ T_{\pi\sigma}(\omega) \end{pmatrix} = \begin{pmatrix} T_{\sigma\sigma}(\omega) & T_{\sigma\pi}(\omega) \\ T_{\pi\sigma}(\omega) & T_{\pi\pi}(\omega) \end{pmatrix} \cdot \begin{pmatrix} 1 & 0 \\ 0 & 0 \end{pmatrix} \cdot \begin{pmatrix} A_\sigma \\ A_\pi \end{pmatrix}. \tag{13}$$

The right hand matrix represents the first polarizer and $\theta = 17°$, $\phi = 0$ is used to calculate $T_{\sigma\sigma}(\omega)$ and $T_{\pi\sigma}(\omega)$. Fig. (3) shows $\vec{A}'(t)$ also considering its polarization direction. At $t = 0$ the polarization is that of the incoming SR pulse (σ polarization). As time goes on the plane of polarization is rotating. However it remains linearly polarized at all times ($T_{\sigma\sigma}(t)$ and $T_{\pi\sigma}(t)$ are real). Further the amplitude is periodically changing, reflecting the

decay and beating of the collective excited state [6].

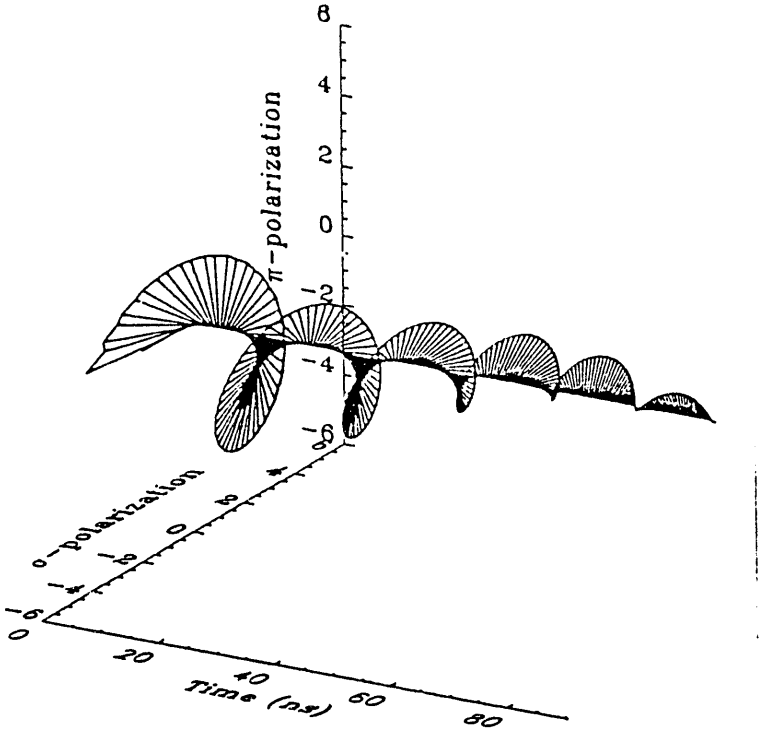

FIGURE 3. Calculated amplitude $\vec{A}'(t)$ of the transmitted wave and its polarization direction during the first 80 *nsec* after excitation. At t=0 the polarization is parallel to the polarization of the SR pulse. The polarization remains linear but rotates in time as the amplitude decreases exponentially showing quantum beats with a 14 *nsec* time period.

To relate this result to a measurable quantity we calculate the time dependent intensity $I(t)$. It is simply proportional to the modulus squared of $\vec{A}'(t)$, i.e. $I(t) = I_{\sigma\sigma}(t) + I_{\pi\sigma}(t)$ and shown as a solid line in Fig. (4). For our experimental conditions the frequency differences of the $\Delta m = +1$ and $\Delta m = -1$ lines are equal and lead to a single beat period of 14 *nsec* in $I(t)$. Fig. (4) also shows the components $I_{\sigma\sigma}(t)$ (dashed) and $I_{\pi\sigma}(t)$ (dotted) seperately. They both show beating, but with twice the frequency of the total intensity beats. This arises because an analyzer imposes additional minima whenever

the polarization of the transmitted wave is perpendicular to its acceptance direction.

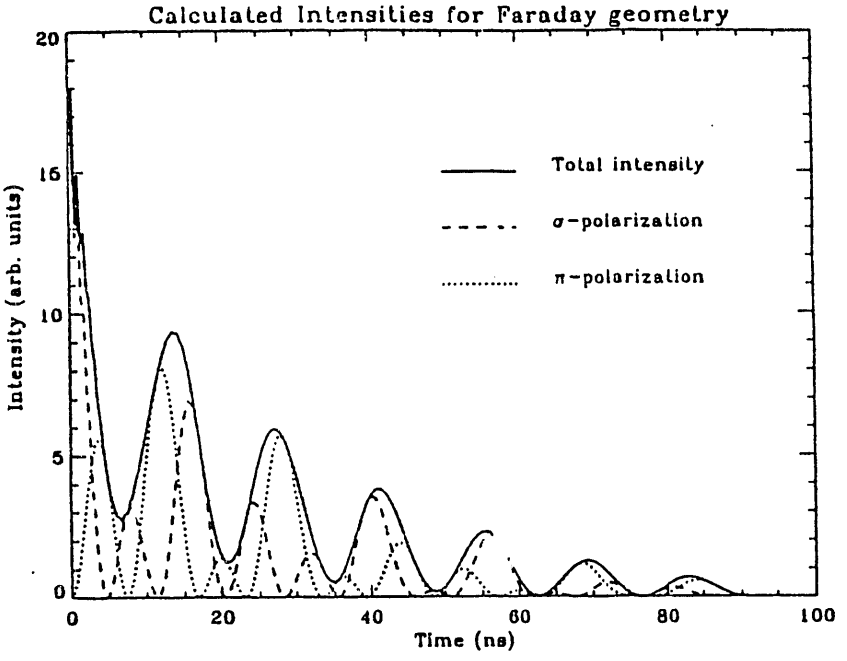

FIGURE 4. Intensity components $I_{\sigma\sigma}(t)$ (dashed line), $I_{\pi\sigma}(t)$ (dotted line) and total intensity $I(t) = I_{\sigma\sigma}(t) + I_{\pi\sigma}(t)$ (solid line), which is the square of the amplitude shown in Fig. (3).

Fig. (5) shows the comparison between our measurement of $I(t)$ without the Be-crystal analyzer and the calculation shown in Fig. (4) (solid line). The sample had a thickness of 0.475 μm and was set to an angle of 17° towards $\hat{k}_0$. The external magnetic field was applied horizontally along the surface to give $\theta = 17°$ and $\phi = 0$. The effective sample thickness was therefore 1.6 μm. The detector was the same as used in previous experiments (see e.g. [21]). The NSLS storage ring operated in five and single bunch mode, which provides a time window of about 80 *nsec* (5 bunch mode) [22]. The time-integrated intensity in the detector was $3.5 \cdot 10^5$ Hz, and the background substracted delayed intensity in our time window (25 - 75 *nsec*) was about 0.5 Hz. This data clearly demonstrates the limitation of a SR-based NFS measurements without electronic suppression. For the first 20 *nsec* the detector cannot recover from the prompt radiation burst. Further any lack of purity in the electron bunch structure results in significant perturbations to the

data as evidenced around 20 and 75 $nsec$ in Fig. (5).

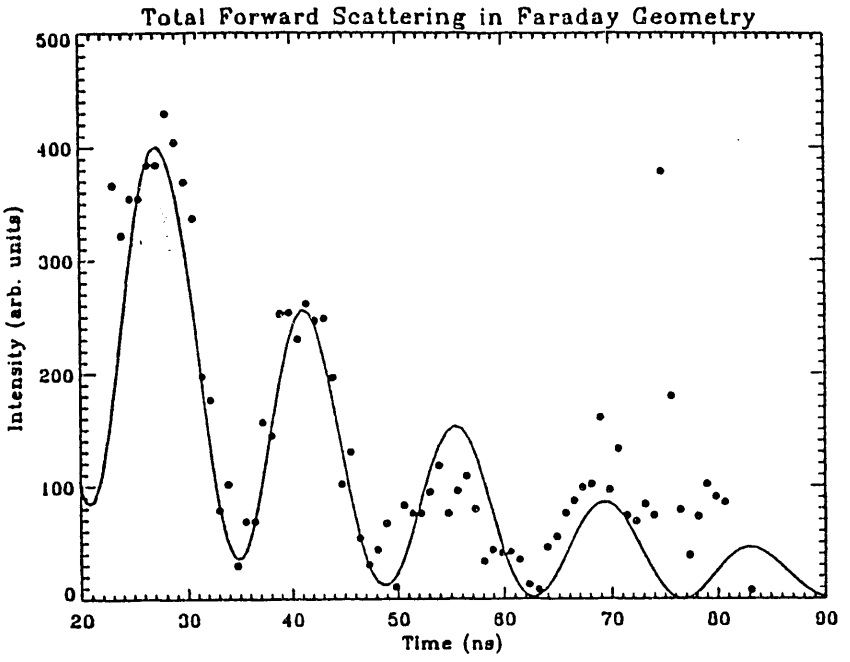

FIGURE 5. Comparison between calculated and measured total intensity. No analyzer is used in this geometry.

To achieve polarization analysis and charge suppression we introduce the Be-crystal analyzer. Now the matrix equation from Fig. (1) applies,

$$\vec{A}'(\omega) = \begin{pmatrix} 0 \\ T_{\pi\sigma}(\omega) \end{pmatrix} = \begin{pmatrix} 0 & 0 \\ 0 & 1 \end{pmatrix} \cdot \begin{pmatrix} T_{\sigma\sigma}(\omega) & T_{\sigma\pi}(\omega) \\ T_{\pi\sigma}(\omega) & T_{\pi\pi}(\omega) \end{pmatrix} \cdot \begin{pmatrix} 1 & 0 \\ 0 & 0 \end{pmatrix} \cdot \begin{pmatrix} A_\sigma \\ A_\pi \end{pmatrix}. \qquad (14)$$

Again the measured quantity is proportional to the modulus squared of $\vec{A}'(t)$ but $\vec{A}'(\omega)$ is given now by eq. (14), i.e. $I(t) = I_{\pi\sigma}(t)$.

Fig. (6) shows a comparison of the calculation with our measurement. The background subtracted delayed countrate was 0.05 Hz in the same time window, which corresponds to a factor ten reduction in the resonant signal. This rate does not include the first intense beat, which we can now observe because the prompt background is strongly suppressed. The time integrated intensity in the detector is only 80 Hz corresponding to a reduction of $4 \cdot 10^3$. Thus, in spite of the limitations of the Be(00.6) analyzer (Bragg angle limits on the extinction and reflectivity limits on intensity), a factor of 400 relative

suppression has been achieved in these measurements.

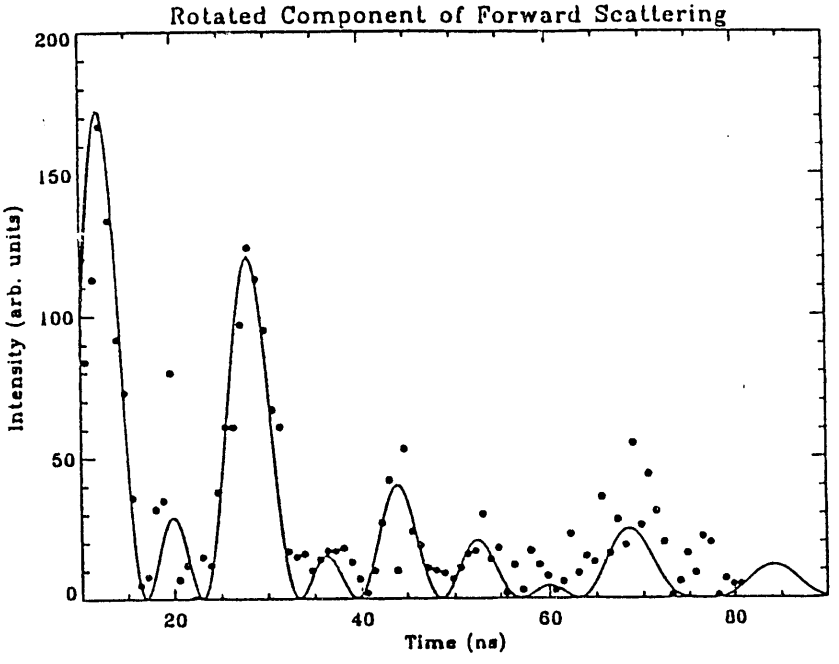

FIGURE 6. Comparison between calculated and measured intensity of the rotated component $I_{\pi\sigma}(t)$. In this geometry the transmitted beam is reflected through 92° by the beryllium crystal, thus suppressing the σ-polarized component (mainly nonresonant prompt scattering).

4. SUMMARY

In this paper we have discussed different techniques of electronic suppression in a SR-based Mössbauer experiment using ^{57}Fe, in particular the suppression method using two crossed polarizers. The basis for this technique is the time-dependent change in polarization of radiation scattered from ^{57}Fe excited by a linearly polarized SR-pulse. Calculations based on the transmission amplitude $\tilde{T}(\omega)$, derived above, are compared to our mesasurements. Our results demonstrate that the unwanted prompt scattering can be reduced by a large factor. In this work we show a suppression of two to three orders of magnitude. In a different context, polarimeter extinctions of order 10^6 have been demonstrated using perfect crystal optics. This technology, which overcomes both limitations of the analyzer used in the present work, is optically well matched to the undulator sources of the next generation facilities.

The experimental setup described in this paper is based on the nuclear Faraday effect. However, polarization mixing is not limited to the Faraday geometry. Given that the

quantization axis can be properly oriented with respect to the incident beam, this technique can be applied as long as the magnitude of the relevant splitting is compatible with the experimental time window. The technique will completely remove detector imposed limits on NFS intensities. The use of crossed polarizers based on perfect Si-crystals seems to be a very promising technique for extending the application of SR-based Mössbauer experiments to different scientific fields. It provides a clean experiment, straightforward data analysis and the possibility of suppression of prompt radiation by at least 10^6.

We also discussed charge suppression achieved with a nuclear filter such as a GIAR-film or an ^{57}Fe enriched crystal. Nuclear filters introduce their own spectral structure to the measurement, limiting one of the major strengths of SR, which is the broadband, short pulse excitation. In general this leads to a complication, although in some cases it might be used as an advantage. The relative suppression achieved with GIAR-films to date is about one order of magnitude. In particular they may be useful for nuclear scattering without any change of polarization (i.e. $\hat{\sigma}$ to $\hat{\sigma}$ scattering) where they represent the only alternative so far.

We would especially like to thank Prof. J. P. Hannon for elucidating the theoretical aspects of this problem and for continuing support and encouragement. We thank Dr. U. van Bürck for discussions and for providing the extremely thin ^{57}Fe sample and L.E. Siddons for the help with the figures. This work is supported by the U.S. Department of Energy under Contract No. DEAC02-76CH00016

References

[a] Current address: Physics department, State University of New York, Stony Brook, New York 11794-3800

[1] F.J. Lynch, R.E. Holland and M. Hammermesh, Phys. Rev. **120**, 513 (1960).

[2] E.J. Seppi and F. Boehm, Phys. Rev. Lett. **128**, 2334 (1962).

[3] S.L. Ruby, J.Phys. (Paris), Colloq. **35**, C6-209 (1974).

[4] W. Sturhahn, E. Gerdau, R. Hollatz, R. Rüffer, H.D. Rüter and W. Tolksdorf, Europhys. Lett. **14** 821 (1991).

[5] E. Gerdau, R. Rüffer, H. Winkler, W. Tolksdorf, C.P. Klages and J.P. Hannon, Phys. Rev. Lett. **54**, 835 (1985).

[6] G.T. Trammel and J.P. Hannon, Phys. Rev. B **18**, 165 (1978).

[7] E. Gerdau, R. Rüffer, R. Hollatz and J.P. Hannon, Phys. Rev. Lett. **57**, 1141 (1986).

[8] S. Kikuta, this conference.

[9] U. van Bürck, R.L. Mössbauer, E. Gerdau, R. Rüffer, R. Hollatz, G.V. Smirnov and J.P. Hannon, Phys. Rev. Lett. **59**, 355 (1987).

[10] G. Faigel, D.P. Siddons, J.B. Hastings, P.E. Haustein, J.R. Grover and L.E. Berman, Phys. Rev. Lett. **61**, 2794 (1988).

[11] G. Faigel, D.P. Siddons, J.B. Hastings, P.E. Haustein, J.R. Grover, J.P. Remeika and A.S. Cooper, Phys. Rev. Lett. **58**, 2699 (1987).

[12] D.P. Siddons, J.B. Hastings, G. Faigel, L.E. Berman, P.E. Haustein and J.R. Grover, Phys. Rev. Lett. **62**, 1384 (1989).

[13] R. Röhlsberger, E. Gerdau, M. Harsdorff, O. Leupold, E. Lüken, J. Metge, R. Rüffer, H.D. Rüter, W. Sturhahn and E. Witthoff Europhys. Lett. **18**, 561 (1992).

[14] S. Hanna, J. Heberle, C. Littlejohn, G.J. Perlow, R.S. Preston, and D.H. Vincent, Phys. Rev. Lett. **4**, 177 (1960a).

[15] E. Hecht, Optics, Second Edition, Addison-Wesley Publishing Company, Inc., 1989.

[16] D.P. Siddons, M. Hart, Y. Amemiya, and J.B. Hastings, Phys. Rev. Lett. **64**, 1967 (1990).

[17] M. Blume and O.C. Kistner, Phys. Rev. **171**, 417, (1968).

[18] J.P. Hannon and G.T. Trammell, Phys. Rev. **186**, 306, (1969).

[19] J. Kagan and A. M. Afanas'ev, Z.Naturfrsch. **28a**, 1351 (1973).

[20] J.P. Hannon, private communications, 1990.

[21] J.B. Hastings, D.P. Siddons, U. van Bürck, R. Hollatz and U. Bergmann, Phys. Rev. Lett. **66**, 770 (1991).

[22] U. van Bürck, D.P. Siddons, J.B. Hastings, U. Bergmann and R. Hollatz, Phys. Rev. B, (1992), in press.

[23] P. Imbert, Physics Letters **8**, number 2 (1964).

[24] U. Gonser and R. M. Hously, Physics Letters, **26A**, 157, (1968).

DATE
FILMED
8/18/93
END